Allergologia et immunopathologia
Sociedad Española de Inmunología Clínica, Alergología y Asma Pediátrica
www.all-imm.com

ORIGINAL ARTICLE

OPEN ACCESS

Identification of biomarkers and candidate small-molecule drugs in lipopolysaccharide (LPS)-induced acute lung injury by bioinformatics analysis

Xu Wang, Bin Chen*, Chao Chen*

Department of Anesthesia, the Ninth People's Hospital Affiliated to Medical School of Shanghai Jiaotong University, Shanghai, China

Received 15 August 2022; Accepted 31 August 2022
Available online: 1 January 2023

KEYWORDS
acute lung injury; bioinformatics analysis; differentially expressed genes; pyridoxal phosphate; *SERPINA3*

Abstract
Background/objective: Acute lung injury (ALI) is a critical clinical syndrome with high rates of incidence and mortality. However, its molecular mechanism remains unclear. The current work aimed to explore the molecular mechanisms of ALI by identifying different expression genes (DEGs) and candidate drugs using a combination of chip analysis and experimental validation.
Methods: Three microarray datasets were downloaded from Gene Expression Omnibus (GEO) database to obtain DEGs. We conducted a Gene Ontology and Kyoto Encyclopedia of Genes and Genomes pathway-enrichment analyses of overlapping DEGs among three databases. The expression level of key gene was verified by Western blotting analysis in LPS-treated ALI cell models. Finally, we predicted the candidate drugs targeting the key gene that might be effective for ALI treatment, and the role of candidate drug in treating ALI was verified by investigation.
Results: A total 29 overlapping DEGs were up-regulated in LPS-induced ALI groups. They were enriched in inflammation and inflammation-related pathways. *Serpin family A member 3* (*SERPINA3*) was defined as a key gene because it was associated with inflammation pathway and up-regulated in microarray datasets in LPS-induced ALI. In LPS-induced human bronchial epithelial cells transformed with Ad12-SV40-2B (BEAS-2B) cells, *SERPINA3* was enhanced. Pyridoxal phosphate as an upstream drug of *SERPINA3* could improve cell viability and reduce expression inflammatory factors in LPS-treated BEAS-2B cells.
Conclusion: Our study suggested that pyridoxal phosphate could be a candidate drug targeting *SERPINA3* gene in LPS-induced ALI. It has protective and anti-inflammatory effects in BEAS-2B cells, and may become a potential novel treatment for ALI.

***Corresponding authors:** Bin Chen and Chao Chen, Department of Anesthesia, the Ninth People's Hospital Affiliated to Medical School of Shanghai Jiaotong University, No. 639, Zhizaoju Road, Shanghai 200011, China. *Email addresses:* bchen7665@163.com (Bin Chen); and dr_chenchao@163.com (Chao Chen)

https://doi.org/10.15586/aei.v51i1.755

Introduction

Acute lung injury (ALI) is regarded as a critically grievous clinical syndrome characterized by increasing capillary permeability, release of inflammatory cytokines, and accumulation of neutrophils in the lungs.[1,2] Many precipitating factors, such as inflammation of the lungs, space-occupying lesions and trauma, etc., and ultimately lead to acute hypoxic respiratory insufficiency or respiratory failure, even acute respiratory distress syndrome (ARDS).[3] Therefore, ALI is a typical clinical disease with high morbidity and mortality rates.[4] Numerous studies have proved that lipopolysaccharide (LPS), the main component of Gram-negative bacteria's outer membrane, may induce lung injury and inflammation.[5,6] For example, Zeng et al. (2017) found that LPS could activate endoplasmic reticulum (ER) stress and enhance the release of pro-inflammatory mediators in alveolar epithelial cells.[7] Hence, treatment of mice or lung cells with LPS is a common strategy of establishing *in vivo* and *in vitro* ALI models which can successfully elicit inflammatory response in lung tissue or cells.[8] Currently, the available treatments for ALI are limited, and the treatment protocols are mainly supportive therapy, such as mechanical ventilation, etiological treatment, and comprehensive treatment, to maintain fluid, electrolyte, acid, and alkali balance.[9,10] Hence, effective therapeutic measures for ALI are still lacking, and its molecular mechanism remains unclear. Thus, there is an urgent requirement to investigate the pathogenesis of ALI.

Recently, development of microarray and sequencing technology has helped to further explore the potential pathological biomarkers involved in ALI.[11] Meanwhile, Gene Expression Omnibus (GEO), a large public database, can be used to screen different expression genes (DEGs) related to the initiation and progression of ALI from microarray data.[3,12] For example, Tu et al. (2021) identified 20 hub-genes up-regulated in ALI by GEO microarray database.[13] These hub-genes were mainly enriched in nuclear factor *kappa B* (NF-κB) and tumor necrosis factor-α (TNF-α) signaling pathway, indicating that they were important pathways affecting the pathogenesis of ALI.[13] It is possible to find potential therapeutic drugs targeting DEGs. Moreover, investigation of drug–genes interactions could yield a fresh concept for treating the disease.[14]

In this study, three microarray datasets were downloaded from GEO datasets for exploring the molecular mechanisms of ALI. Subsequently, overlapping DEGs were identified and functional enrichment analysis was performed. Finally, Serpin family A member 3 (*SERPINA3*) that has been reported to be dysregulated in lung injury was selected as a key gene. Meanwhile, the QuartataWeb server (http://quartata.csb.pitt.edu/) was used to predict and verify small molecule drugs that may overcome ALI by targeting *SERPINA3*.

Materials and Methods

GEO data

Three independent gene expression analyses (GSE2411, GSE17355, and GSE162354) were downloaded from the GEO database (https://www.ncbi.nlm.nih.gov/geo/) to identify DEGs. The microarray data of GSE2411 was based on GPL339 platform ([MOE430A] Affymetrix Mouse Expression 430A Array) and included six wild-type C57/B6 mice as control groups, and six wild-type mice injected intraperitoneally with LPS as ALI groups. The GSE17355 dataset was based on GPL4865 platform (Sentrix MouseRef-8 Expression BeadChip) and included three wild-type mice models of ALI. GSE162354 dataset was based on GPL21103 platform (Illumina HiSeq 4000 [Mus musculus]) and included six control groups and six LPS treatment lung endothelial cells.

Data processing and identification of DEGs

Raw data were processed and analyzed using the R software (version 4.1.2). Prior to analyzing DEGs in ALI, the sequence data were normalized using normalize Between Arrays. Then, Limma package was performed to analyze DEGs with a cutoff $P < 0.05$ and $|logFC| \geq 1$. The volcano plot and heat map were drawn by ggplot2 program and pheatmap R package, respectively. Then, Venn diagram analysis was performed to find overlapping DEGs in three datasets, and the Venn diagram was drawn by BioLadder online software (www.bioladder.cn/web/#/pro/index).

Gene ontology (GO) and Kyoto Encyclopedia of Genes and Genomes (KEGG)-enrichment analyses

In order to analyze the potential processes and pathway of common DEGs, we used the online software Metascape (http://metascape.org/) to perform GO–KEGG pathway-enrichment analysis, which is a friendly and reliable tool for functional enrichment analysis.[15] The cutoff value of overlap was 3, enrichment was 1.5, and $P < 0.05$ was considered statistically significant. Bubble chart and circle diagrams were drawn by BioLadder (https://www.bioladder.cn/web/#/pro/index), an online mapping software.[16]

Prediction of candidate small molecule drugs

The candidate small molecule drugs targeting *SERPINA3* were predicted by QuartataWeb server; it allows users to query a series of chemicals, drug combinations, or multiple targets to enable multi-drug, multi-target, and multi-pathway analyses toward facilitating the design of polypharmacological treatments for complex diseases.[17] Pyridoxal phosphate (MC-1) has anti-inflammatory effects and can be used as a treatment option for diseases such as cerebral ischemia, and we choose it for the following experiments. The structural formula of pyridoxal phosphate was obtained from PubChem.[18]

Cell culture and treatment

Human bronchial epithelial cells transformed with Ad12-SV40-2B (BEAS-2B) were acquired from American Type Culture Collection (ATCC, VA, USA). BEAS-2B cells were incubated in Dulbecco's Modified Eagle *Medium* (DMEM; Life Technologies, MA, USA) with 10% fetal bovine serum and

1% penicillin–streptomycin antibiotics in a humidified incubator at 37°C with 5% carbon dioxide (CO_2).

Tomimic cell models of ALI, BEAS-2B, were treated with 2.5-, 5-, and 10-mg/L LPS (Sigma-Aldrich, USA) for 24 h.

In order to assess whether pyridoxal phosphate could cause cytotoxicity in BEAS-2B cells, the cells were treated with 6.25-, 12.5-, 25-, and 50-μM pyridoxal phosphate (Sigma-Aldrich, MA. USA) for 24 h, and cell viability was tested by MTT assay.

In order to determine whether pyridoxal phosphate could reduce cell damage, BEAS-2B cells were exposed to different doses of pyridoxal phosphate (6.25, 12.5, and 25 M) in the presence of LPS (10 mg/L) for 24 h.

Cell viability analysis

3×10^3 BEAS-2B cells were plated into each well of a 96-well plate. The cells were cultivated for 24 h, and then exposed to various concentrations of LPS and pyridoxal phosphate for 24 h. Next, 20 mL of MTT (Sigma-Aldrich) solution (5 mg/mL) was added to each well, and the cells were incubated at 37°C for 4 h. At the indicated time, 150-μL/well dimethyl sulfoxide (DMSO; Sigma-Aldrich) was added to dissolve insoluble formazan products after removing the supernatant. Absorbance (Abs) in different groups detected at 570 nm was measured by microplate reader (Bio-Rad, CA, USA). In the blank group, the well contained medium only, and cells without any treatment were used as a control group. Finally, cell viability was calculated as reported by Ma et al. (2021).[19]

Enzyme-linked immunosorbent serologic assay (ELISA)

In order to detect the content of Interleukin (IL)-1β (cat. No. ab214025), IL-6 (cat. No. ab178013), and tumor necrosis factor-α (TNF-α; cat. No. ab181421) in cells, ELISA kits were used following the manufacturer's protocols (Abcam, Cambridge, UK). The absorbance values were measured at 450 nm using a microplate spectrophotometer (Tecan, Zürich, Switzerland). The contents of IL-1β, IL-6, and TNF-α were calculated according to standard curves.

Western blotting analysis

Different groups of cells were washed with phosphate-buffered saline (PBS) solution for three times, and radioimmunoprecipitation assay buffer (RIPA; Beyotime, Shanghai, China) was used to extract total protein. Protein concentration was determined using a bicinchoninic acid (BCA) protein assay kit (Beyotime). After boiling for 5 min at 95°C in a 5× loading buffer, an equal amount of protein was separated with 10% sodium dodecyl sulfate–polyacrylamide gel electrophoresis (SDS-PAGE). Then, these were transferred to polyvinylidene fluoride (PVDF) membranes (Millipore, Beijing, China) and treated with 5% non-fat milk for 1 h at room temperature. The protein was identified by incubation with specific primary antibodies anti-*SERPINA3* (ab205198, 1:2000) and anti-β-actin (ab8227, 1:2000) overnight at 4°C. All the antibodies were bought from Abcam. The following day, membranes were washed thrice in tris buffered saline with Tween-20 (TBST), and incubated with horseradish peroxidase (HRP)-conjugated secondary immunoglobulin G (IgG) antibody (ab205718, 1:2000; Abcam) for 1 h at room temperature. Before imaging, the membranes were washed thrice with TBST, and enhanced chemiluminescence (ECL) reagent (Beyotime) was used for detection of expressed proteins.

Statistical analysis

The mean value and standard deviation (SD) from three different experiments were used to represent the data. For statistical analysis, GraphPad Prism 7.04 was used. For comparing two groups, Student's *t*-test was employed, and for comparing multiple groups, one-way ANOVA was used. Statistically, $P < 0.05$ was considered significant.

Results

Identification of DEGs in acute lung injury by multi-microarray combined analysis

To explore molecular biological mechanism of ALI, we downloaded microarray data from the GEO database. Then, Limma package of R software was used for normalization of data. Boxplots shown in Figures 1A–C are correction diagrams of data preprocessing. Volcano plots of each gene expression profile data are also shown in Figures 1A–C. We identified 264 DEGs (245 up-regulated and 19 down-regulated) from GSE2411 dataset, 444 DEGs (315 up-regulated and 129 down-regulated) from GSE17355 dataset, and 2091 DEGs (1051 up-regulated and 1040 down-regulated) from GSE162354 dataset. The heat map demonstrated the expression levels of DEGs in three datasets shown in Figures 1A–C. Next, Venn diagram analysis found that only 29 overlapping DEGs were up-regulated among the three DEG profiles (Figure 1D). Collectively, our data identified 29 DEGs up-regulated in LPS-treated ALI compared with control groups.

Functional enrichment analysis of 29 overlapping DEGs

Gene ontology annotation and KEGG pathways-enrichment analyses were performed through metascape database. The GO analysis revealed that leukocyte chemotaxis and inflammatory response were enriched in 29 overlapped DEGs (Figure 2A). Meanwhile, the KEGG analysis revealed that IL-17 signaling pathway and cytokine–cytokine receptor interaction pathway were enriched in 29 overlapping DEGs (Figure 2B). The top five significantly enriched GO terms and related genes are shown in Table 1 and Figure 2C. We found that *SERPINA3* was one of the related genes that was enriched in leukocyte chemotaxis and inflammatory response. Additionally, since there were less reports of *SERPINA3* in ALI, we employed this gene in the subsequent steps of the study.

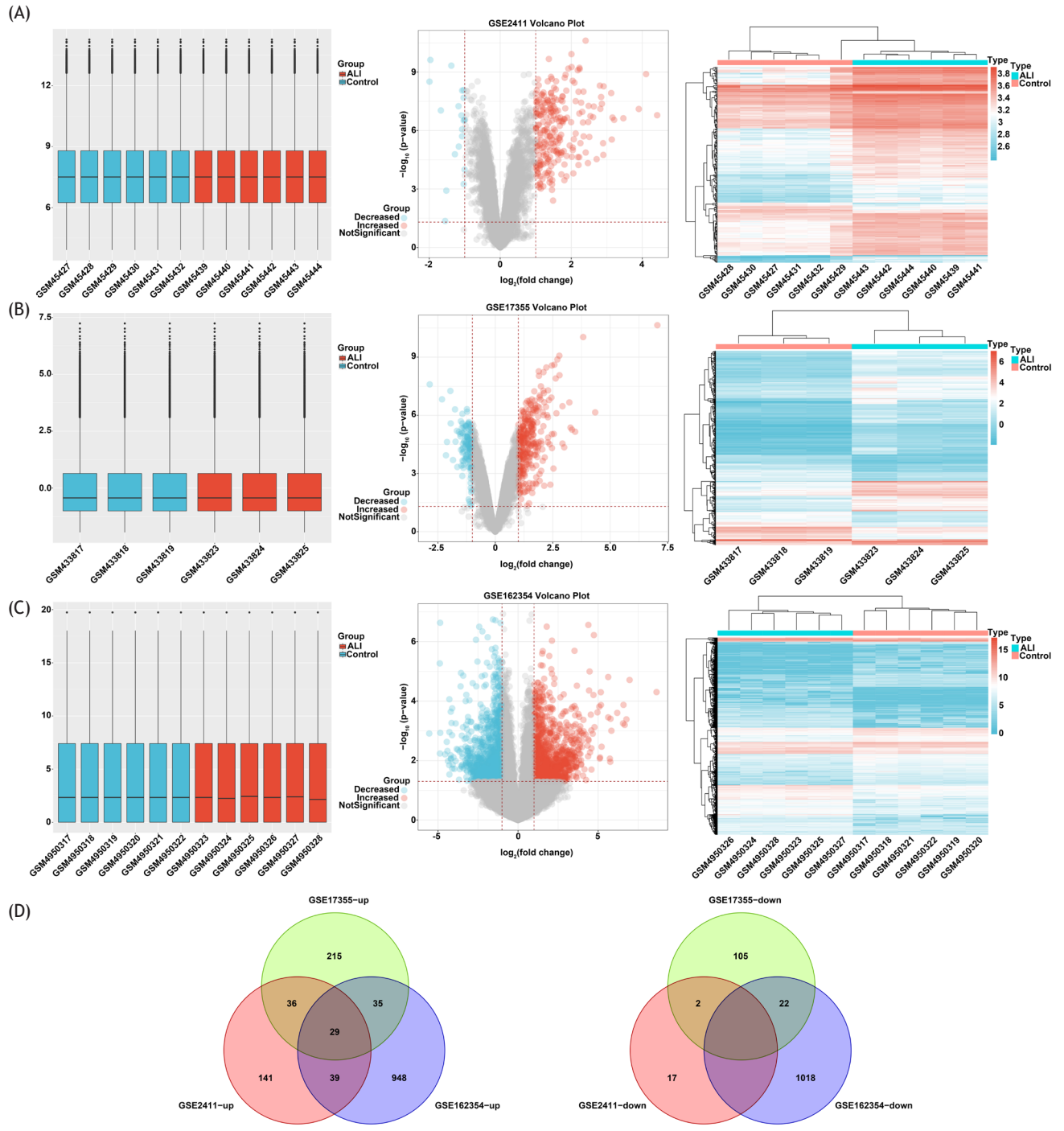

Figure 1 Identification of DEGs in ALI by multi-microarray combined analysis. (A) Boxplots of data normalization, volcano plot and heat maps of DEGs in GSE2411 database; (B) boxplots of data normalization, volcano plot and heat maps of DEGs in GSE17355 database; (C) boxplots of data normalization, volcano plot and heat maps of DEGs in GSE162354 database. The expression level of vertical coordinate represents the expression value after batch normalization of the original data of GEO database; (D) Venn diagram of up-regulated and down-regulated DEGs based on three GEO datasets.

SERPINA3 was up-regulated in LPS-treated BEAS-2B

Here, we first explored the expression of *SERPINA3* in microarray datasets. We compared the expression of three *SERPINA3* gene isoforms (*serpina3n*, *serpina3m*, and *serpina3g*) in the three microarray datasets shown in Figure 3A, and found that the expression of *serpina3n*, *serpina3m*, and *serpina3g* in LPS-treated ALI was up-regulated compared to those in normal state. Next, BEAS-2B cells were exposed to various doses of LPS to simulate the cell model of ALI. As shown in Figure 3B, the protein level of

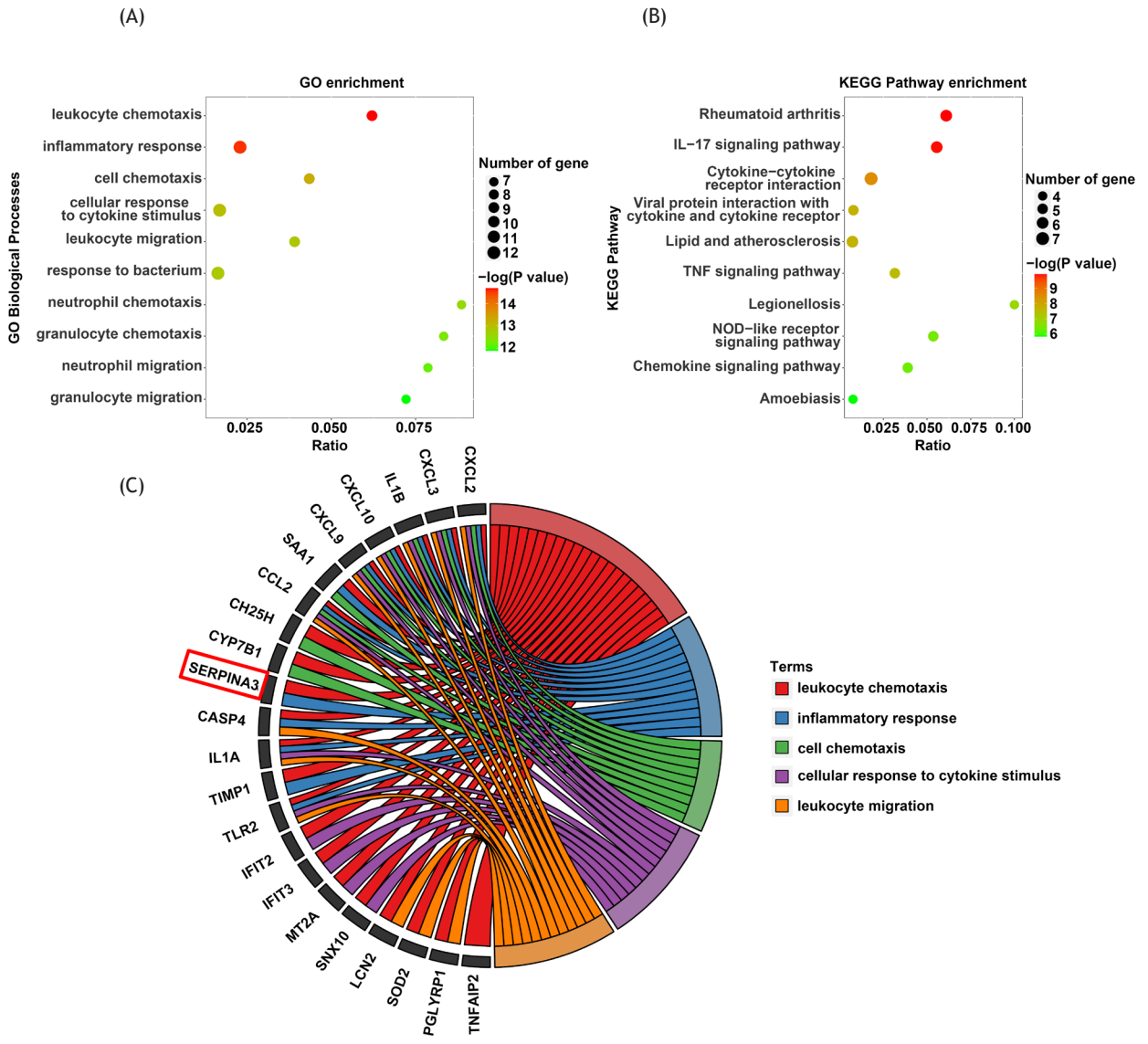

Figure 2 Functional enrichment analysis of 29 overlapping DEGs. (A) GO analysis of 29 up-regulated overlapping DEGs; (B) KEGG analysis of 29 up-regulated overlapping DEGs; (C) circle diagram of top five significantly enriched GO terms and related genes.

SERPINA3 was significantly increased in LPS-treated BEAS-2B in a dosage-dependent manner ($P < 0.05$). Therefore, we determined *SERPINA3* as the key gene for further study.

Pyridoxal phosphate was the candidate small molecule drug targeting SERPINA3

We sought to find therapeutic drugs targeting *SERPINA3* in order to provide therapeutic options. The QuartataWeb server was used for searching potential drugs targeting *SERPINA3*. We identified 22 small molecule drugs targeting *SERPINA3* (Figure 4A). Pyridoxal phosphate was one of the potential drugs targeting *SERPINA3*, and its structural formula is shown in Figure 4B.

Next, we simply measured the protective effects of pyridoxal phosphate on LPS-treated BEAS-2B cells. Treatment with pyridoxal phosphate in a concentration range of 6.25–25 μM did not affect the cell viability of BEAS-2B cells, indicating that pyridoxal phosphate in the stated concentration range was less cytotoxic to BEAS-2B cells (Figure 5A). Then, BEAS-2B cells were stimulated with 10-mg/L LPS for 24 h. MTT assay demonstrated that pyridoxal phosphate in a concentration of 25 μM could significantly improve cell viability of BEAS-2B cells cotreated with LPS ($P < 0.001$; Figure 5B).

In order to explore the anti-inflammatory effect of pyridoxal phosphate, we measured inflammatory factors by ELISA. As shown in Figure 5C, pyridoxal phosphate could decrease the levels of IL-1β, IL-6, and TNF-α in BEAS-2B cells exposed to LPS. Finally, treatment with pyridoxal phosphate could significantly suppress LPS-induced increase in SERPINA3 protein expression (Figure 5D). These results hinted that pyridoxal phosphate could induce cell survival and inhibit inflammation in LPS-treated BEAS-2B by targeting *SERPINA3*.

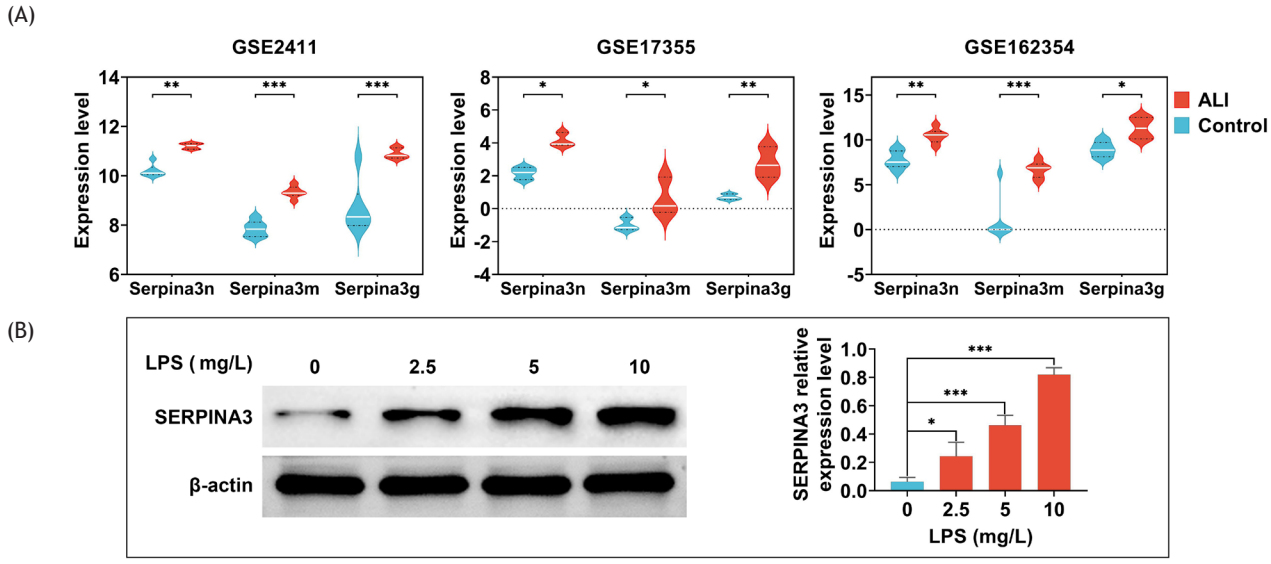

Figure 3 SERPINA3 was up-regulated in lipopolysaccharide-treated BEAS-2B. (A) The expression of three SERPINA3 gene isoforms (serpina3n, serpina3m, and serpina3g) in GSE2411, GSE17355, and GSE162354 GEO datasets. The expression level of vertical coordinate represents expression value after batch normalization of original data in GEO database; (B) the protein level of SERPINA3 in LPS-treated BEAS-2B cells by Western blotting analysis. Data are representative of three independent experiments (mean ± SD). *P < 0.05, -P < 0.01, ***P < 0.001.

Table 1 Process information of top five GO terms and related genes.

Category	Term	Description	Log P	Log (q-value)	InTerm_InList	Symbols
GO biological processes	GO: 0030595	Leukocyte chemotaxis	−14.6949	−10.518	9/145	CXCL2, CXCL3, IL1B, CXCL10, CXCL9, SAA1, CCL2, CH25H, CYP7B1, SERPINA3, CASP4, IL1A, TIMP1, TLR2, IFIT2, IFIT3, MT2A, SNX10, LCN2, SOD2, PGLYRP1, TNFAIP2
GO biological processes	GO: 0006954	Inflammatory response	−14.5648	−10.518	12/523	SERPINA3, CASP4, CXCL2, CXCL3, IL1A, IL1B, CXCL10, CXCL9, SAA1, CCL2, TIMP1, TLR2
GO biological processes	GO: 0060326	Cell chemotaxis	−13.283	−9.412	9/207	CXCL2, CXCL3, IL1B, CXCL10, CXCL9, SAA1, CCL2, CH25H, CYP7B1
GO biological processes	GO: 0071345	Cellular response to cytokine stimulus	−12.99	−9.331	12/710	CXCL2, CXCL3, IFIT2, IFIT3, IL1A, IL1B, CXCL10, CXCL9, MT2A, CCL2, TLR2, SNX10
GO biological processes	GO: 0050900	Leukocyte migration	−12.8682	−9.331	9/230	CXCL2, CXCL3, IL1B, CXCL10, CXCL9, SAA1, CCL2, CH25H, CYP7B1

Discussion

Owing to its complex etiology and poorly understood pathophysiology, ALI has not been established considerably. Hence, investigation of molecular mechanism of ALI is an urgent task.[20] Recent developments of microarray technology have further explored the potential pathological biomarkers of many diseases, including ALI.[21] In this study, we used three microarray datasets (GSE2411, GSE17355, and GSE162354) downloaded from GEO datasets to screen DEGs in LPS-induced ALI. A total of 29 genes were common DEGs in these three datasets, which were up-regulated in ALI groups compared to those in control groups. Additionally, to explore the potential molecular mechanisms of ALI that might underlie the therapeutic effect, we used metascape database to conduct GO-KEGG-enrichment analysis. For GO-enrichment analysis, 29 overlapping DEGs were enriched in leukocyte chemotaxis and inflammatory response (Figure 2A). Most data indicated that inflammatory storm is the key factor in the occurrence of ALI,[22] and release of pro-inflammatory cytokines, such as IL-1β, TNF-α, and IL-6, were found in the lung tissues of ALI mice models and aggravated lung injury.[23,24] In addition, leukocyte invasion also emerged in LPS-induced lung tissues to induce a robust inflammatory reaction.[25] The results of GO analysis in this study were

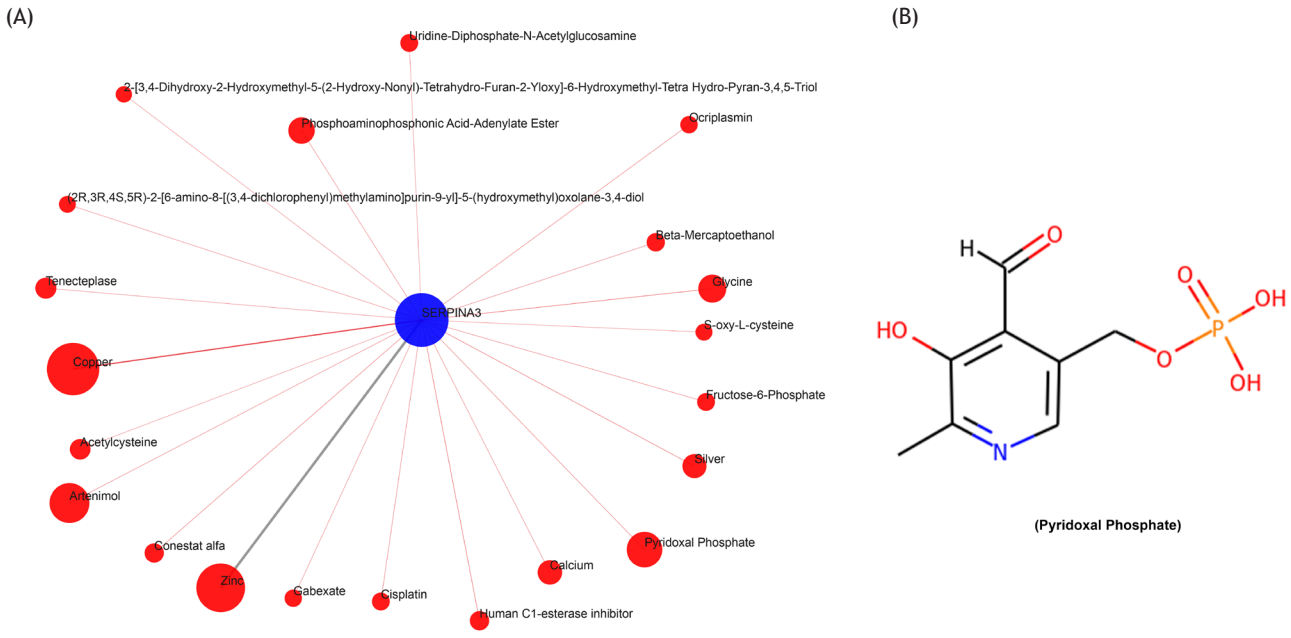

Figure 4 Compound-genomics target drug prediction for SERPINA3. (A) Compounds of targeted SERPINA3 were predicted by QuartataWeb; (B) the structural formula of pyridoxal phosphate was predicted by PubChem.

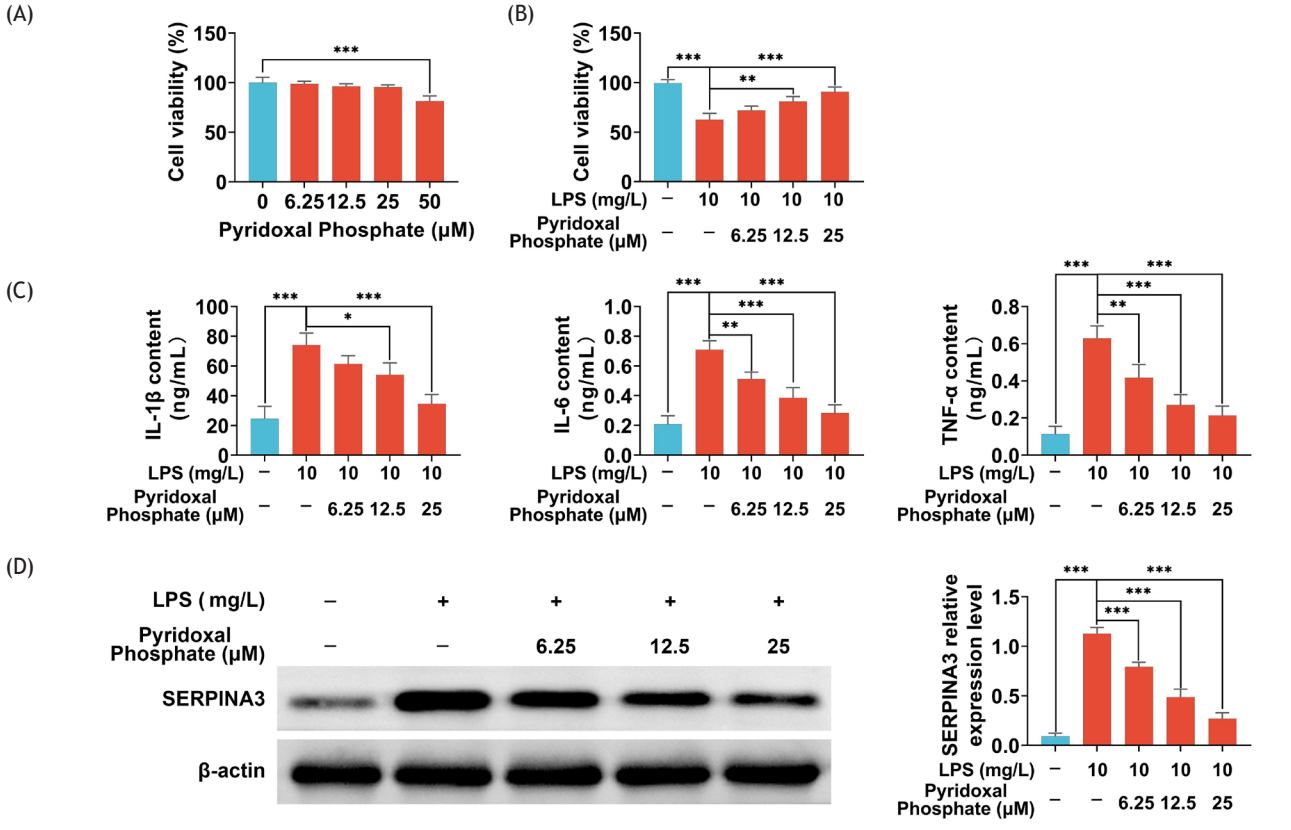

Figure 5 Pyridoxal phosphate-regulated cell viability and inflammation in LPS-treated BEAS-2B cells. (A) Cell viability of BEAS-2B cells with different concentrations of pyridoxal phosphate treatment was measured by MTT assay; (B) cell viability of LPS-treated BEAS-2B cells treated with or without pyridoxal phosphate was measured by MTT assay; (C) concentrations of IL-1β, IL-6, and TNF-α in LPS-treated BEAS-2B cells treated with or without pyridoxal phosphate were measured by ELISA; (D) protein level of SERPINA3 in LPS-treated BEAS-2B cells treated with or without pyridoxal phosphate was measured by Western blotting assay. Data are representative of three independent experiments (mean ± SD). *P < 0.05, **P < 0.01, ***P < 0.001.

confirmed by the results of cited studies. The results of KEGG pathway analysis proved that IL-17 signaling pathway was enriched among 29 overlapping DEGs. IL-17 acted by activating inducible nitric oxide synthase (iNOS) and inducing the expression of macrophage and several chemokines which collaborated to potentiate inflammatory process.[26] Liao et al. (2021) reported that IL-17 could promote ventilator-induced lung injury via activation of p38 mitogen-activated protein kinase (MAPK)–*monocyte chemoattractant protein*-1 (MCP-1) pathway.[27] Taken together, inflammation and inflammation-related pathways played an important role in the development of ALI. Next, we found that 12 genes (*SERPINA3*, *CASP4*, *CXCL2*, *CXCL3*, *IL1A*, *IL1B*, *CXCL10*, *CXCL9*, *SAA1*, *CCL2*, *TIMP1*, and *TLR2*) were associated with inflammatory response (GO: 0006954). Indeed, expression of *SERPINA3* has been reported to be dysregulated in models of radiation-induced lung injury (RILI), and increased protein expression of *SERPINA3* has been observed in bronchoalveolar lavage and plasma samples.[28] In addition, Uysal et al. (2019) found that *SERPINA3* was highly expressed in the plasma of chronic obstructive pulmonary disease (COPD) patients, and the increased expression of *SERPINA3* might play an important role in airway remodeling in the pathogenesis of COPD.[29] Hence, *SERPINA3*, which has been reported in lung injury and other related lung diseases, as well as associated with inflammatory response, was chosen as a key gene for further research in this study.

SERPINA3, also known as alpha-1 antichymotrypsin, acts as an inhibitor of several serine proteases.[30] Numerous studies have strengthened the idea that *SERPINA3* might function as a possible biomarker in several inflammatory illnesses. For example, increased *SERPINA3* levels were seen in ulcerative colitis. Silencing of *SERPINA3* attenuated inflammation status in TNF-α-treated intestinal epithelial cells.[30] Increased plasma levels of *SERPINA3* were found in coronary artery disease (CAD). Overexpression of *SERPINA3* can enhance the expression of inflammatory markers in human umbilical vein endothelial cells (HUVEC), proving its important role in CAD.[31] In the present study, three *SERPINA3* gene isoforms (*serpina3n*, *serpina3m*, and *serpina3g*), in three microarray datasets, were up-regulated in ALI compared to those in control groups. Additionally, our results also confirmed that SERPINA3 protein was increased in BEAS-2B cells treated with LPS, and these results further demonstrated that *SERPINA3* could be associated with ALI.

In order to investigate the potential therapeutic agents for ALI, QuartataWeb server was used for searching potential drugs targeting *SERPINA3*. Pyridoxal phosphate was one of the potential drugs targeting *SERPINA3*. Previous studies have indicated that pyridoxal phosphate has anti-inflammatory effects,[32,33] and can be used as a therapeutic option for diseases such as cerebral ischemia.[34] However, it's effect was not reported in ALI. We performed this investigation to prove that pyridoxal phosphate had protective effects on LPS-treated BEAS-2B cells. Pyridoxal phosphate not only can improve cell viability and decrease inflammatory factors in BEAS-2B cells treated with LPS by targeting *SERPINA3* but also can decrease SERPINA3 protein level. However, the underlying functional regulatory mechanism needs further investigation, such as whether *SERPINA3* regulates downstream-related signaling pathways, and whether *SERPINA3* can be related to apoptosis, autophagy, iron death, pyroptosis, and so on. In addition, experiments must further elaborate the protective effect of pyridoxal phosphate and *SERPINA3* in ALI animal models.

Conclusion

We used GEO microarray datasets to screen DEGs in LPS-induced ALI, and discovered that *SERPINA3*, a key gene, was increased in LPS-induced BEAS-2B cells. Pyridoxal phosphate as an upstream drug for *SERPINA3* had protective and anti-inflammatory effects on LPS-treated BEAS-2B cells. These results illustrated that pyridoxal phosphate–*SERPINA3* could become a candidate novel treatment targeting ALI.

Competing Interests

The authors stated that there were no conflict of interest to disclose.

Ethics Approval

This study had no investigation with human participants or animals performed by any of the authors.

Data Availability

The authors declare that all data supporting the findings of this study are available within the paper and any raw data can be obtained from the corresponding authors upon request.

Author Contribution

Xu Wang, Bin Chen, and Chao Chen designed and conducted the study. All the authors supervised data collection, and analyzed, interpreted, and prepared the manuscript for publication. Finally, all the authors reviewed the draft, and read and approved the final manuscript.

References

1. Ruoyang Z, Bonda. WLM, Matute-bello. G, Jabaudon M. From preclinical to clinical models of acute respiratory distress syndrome. Signa Vitae. 2022;18(1):3–14. https://doi.org/10.22514/sv.2021.228
2. Meiyan W, Qian C. Phillygenin attenuates LPS-induced acute lung injury of newborn mice in infantile pneumonia. Signa Vitae. 2021;17(4):171–7. https://doi.org/10.22514/sv.2021.085
3. Cao F, Wang C, Long D, Deng Y, Mao K, Zhong H. Network-based integrated analysis of transcriptomic studies in dissecting gene signatures for LPS-induced acute lung injury. Inflammation. 2021;44(6):2486–98. https://doi.org/10.1007/s10753-021-01518-8
4. Wang C, Yuan W, Hu A, Lin J, Xia Z, Yang CF, et al. Dexmedetomidine alleviated sepsis-induced myocardial ferroptosis and septic heart injury. Mol Med Rep. 2020;22(1):175–84. https://doi.org/10.3892/mmr.2020.11114

5. Hsieh YH, Deng JS, Pan HP, Liao JC, Huang SS, Huang GJ. Sclareol ameliorate lipopolysaccharide-induced acute lung injury through inhibition of MAPK and induction of HO-1 signaling. Int Immunopharmacol. 2017;44:16–25. https://doi.org/10.1016/j.intimp.2016.12.026
6. Kolomaznik M, Nova Z, Calkovska A. Pulmonary surfactant and bacterial lipopolysaccharide: The interaction and its functional consequences. Physiol Res. 2017;66(Suppl 2):S147–57. https://doi.org/10.33549/physiolres.933672
7. Zeng M, Sang W, Chen S, Chen R, Zhang H, Xue F, et al. 4-PBA inhibits LPS-induced inflammation through regulating ER stress and autophagy in acute lung injury models. Toxicol Lett. 2017;271:26–37. https://doi.org/10.1016/j.toxlet.2017.02.023
8. Liu P, Feng Y, Li H, Chen X, Wang G, Xu S, et al. Ferrostatin-1 alleviates lipopolysaccharide-induced acute lung injury via inhibiting ferroptosis. Cell Mol Biol Lett. 2020;25:10. https://doi.org/10.1186/s11658-020-00205-0
9. Li J, Lu K, Sun F, Tan S, Zhang X, Sheng W, et al. Panaxydol attenuates ferroptosis against LPS-induced acute lung injury in mice by Keap1-Nrf2/HO-1 pathway. J Transl Med. 2021;19(1):96. https://doi.org/10.1186/s12967-021-02745-1
10. Mokrá D. Acute lung injury—From pathophysiology to treatment. Physiol Res. 2020;69(Suppl 3):S353–66. https://doi.org/10.33549/physiolres.934602
11. Niethamer TK, Stabler CT, Leach JP, Zepp JA, Morley MP, Babu A, et al. Defining the role of pulmonary endothelial cell heterogeneity in the response to acute lung injury. eLife. 2020;9:e53072. https://doi.org/10.7554/eLife.53072
12. Vogelstein B, Papadopoulos N, Velculescu VE, Zhou S, Diaz LA, Jr., Kinzler KW. Cancer genome landscapes. Science (New York, NY). 2013;339(6127):1546–58. https://doi.org/10.1126/science.1235122
13. Tu Q, Zhu Y, Yuan Y, Guo L, Liu L, Yao L, et al. Gypenosides inhibit inflammatory response and apoptosis of endothelial and epithelial cells in LPS-induced ALI: A study based on bioinformatic analysis and in vivo/vitro experiments. Drug Design Dev Ther. 2021;15:289–303. https://doi.org/10.2147/DDDT.S286297
14. Rahal Z, El Nemr S, Sinjab A, Chami H, Tfayli A, Kadara H. Smoking and lung cancer: A Geo-regional perspective. Front Oncol. 2017;7:194. https://doi.org/10.3389/fonc.2017.00194
15. Zhou Y, Zhou B, Pache L, Chang M, Khodabakhshi AH, Tanaseichuk O, et al. Metascape provides a biologist-oriented resource for the analysis of systems-level datasets. Nature Commun. 2019;10(1):1523. https://doi.org/10.1038/s41467-019-09234-6
16. Ye Y, Jin Q, Gong Q, Li A, Sun M, Jiang S, et al. Bioinformatics and experimental analyses reveal NFIC as an upstream transcriptional regulator for ischemic cardiomyopathy. Genes. 2022;13(6):1051. https://doi.org/10.3390/genes13061051
17. Li H, Pei F, Taylor DL, Bahar I. QuartataWeb: Integrated chemical-protein-pathway mapping for polypharmacology and chemogenomics. Bioinformatics (Oxford, England). 2020;36(12):3935–7. https://doi.org/10.1093/bioinformatics/btaa210
18. Kim S, Chen J, Cheng T, Gindulyte A, He J, He S, et al. PubChem in 2021: New data content and improved web interfaces. Nucleic Acids Res. 2021;49(D1):D1388–95. https://doi.org/10.1093/nar/gkaa971
19. Ma LY, Liu JM, Du GL, Dang XB. Irisin attenuates lipopolysaccharide-induced acute lung injury by downregulating inflammatory cytokine expression through miR-199a-mediated Rad23b overexpression. Exp Cell Res. 2021;404(2):112593. https://doi.org/10.1016/j.yexcr.2021.112593
20. Butt Y, Kurdowska A, Allen TC. Acute lung injury: A clinical and molecular review. Arch Pathol Lab Med. 2016;140(4):345–50. https://doi.org/10.5858/arpa.2015-0519-RA
21. Mao K, Geng W, Liao Y, Luo P, Zhong H, Ma P, et al. Identification of robust genetic signatures associated with lipopolysaccharide-induced acute lung injury onset and astaxanthin therapeutic effects by integrative analysis of RNA sequencing data and GEO datasets. Aging. 2020;12(18):18716–40. https://doi.org/10.18632/aging.104042
22. Grommes J, Soehnlein O. Contribution of neutrophils to acute lung injury. Mol Med (Cambridge, MA). 2011;17(3–4):293–307. https://doi.org/10.2119/molmed.2010.00138
23. Wang J, Cai X, Ma R, Lei D, Pan X, Wang F. Anti-inflammatory effects of Sweroside on LPS-induced ALI in mice via activating SIRT1. Inflammation. 2021;44(5):1961–8. https://doi.org/10.1007/s10753-021-01473-4
24. Song C, Li H, Li Y, Dai M, Zhang L, Liu S, et al. NETs promote ALI/ARDS inflammation by regulating alveolar macrophage polarization. Exp Cell Res. 2019;382(2):111486. https://doi.org/10.1016/j.yexcr.2019.06.031
25. Ehrentraut H, Weisheit CK, Frede S, Hilbert T. Inducing acute lung injury in mice by direct intratracheal lipopolysaccharide instillation. J Vis Exp JoVE. 2019 Jul 6;(149). https://doi.org/10.3791/59999
26. Gonçalves-de-Albuquerque SDC, Pessoa ESR, Trajano-Silva LAM, de Goes TC, de Morais RCS, da COCN, et al. The equivocal role of Th17 cells and neutrophils on immunopathogenesis of leishmaniasis. Front Immunol. 2017;8:1437. https://doi.org/10.3389/fimmu.2017.01437
27. Liao X, Zhang W, Dai H, Jing R, Ye M, Ge W, et al. Neutrophil-derived IL-17 promotes ventilator-induced lung injury via p38 MAPK/MCP-1 pathway activation. Front Immunol. 2021;12:768813. https://doi.org/10.3389/fimmu.2021.768813
28. Thakur P, DeBo R, Dugan GO, Bourland JD, Michalson KT, Olson JD, et al. Clinicopathologic and transcriptomic analysis of radiation-induced lung injury in nonhuman primates. Int J Radiat Oncol Biol Phy. 2021;111(1):249–59. https://doi.org/10.1016/j.ijrobp.2021.03.058
29. Uysal P, Uzun H. Relationship between circulating Serpina3g, matrix metalloproteinase-9, and tissue inhibitor of metalloproteinase-1 and -2 with chronic obstructive pulmonary disease severity. Biomolecules. 2019;9(2):62. https://doi.org/10.3390/biom9020062
30. Zhang J, Wang W, Zhu S, Chen Y. Increased SERPINA3 level is associated with ulcerative colitis. Diagnostics (Basel, Switzerland). 2021;11(12):2371. https://doi.org/10.3390/diagnostics11122371
31. Li B, Lei Z, Wu Y, Li B, Zhai M, Zhong Y, et al. The association and pathogenesis of SERPINA3 in coronary artery disease. Front Cardiovasc Med. 2021;8:756889. https://doi.org/10.3389/fcvm.2021.756889
32. Kandzari DE, Dery JP, Armstrong PW, Douglas DA, Zettler ME, Hidinger GK, et al. MC-1 (pyridoxal 5'-phosphate): Novel therapeutic applications to reduce ischaemic injury. Expert Opin Investig Drugs. 2005;14(11):1435–42. https://doi.org/10.1517/13543784.14.11.1435
33. Thériault O, Poulin H, Thomas GR, Friesen AD, Al-Shaqha WA, Chahine M. Pyridoxal-5'-phosphate (MC-1), a vitamin B6 derivative, inhibits expressed P2X receptors. Can J Physiol Pharmacol. 2014;92(3):189–96. https://doi.org/10.1139/cjpp-2013-0404
34. Wang CX, Yang T, Noor R, Shuaib A. Role of MC-1 alone and in combination with tissue plasminogen activator in focal ischemic brain injury in rats. J Neurosurg. 2005;103(1):165–9. https://doi.org/10.3171/jns.2005.103.1.0165

Supplementary

Table S1 List of 29 overlapping DEGs in three GEO databases (LPS vs. control)

	GSE2411		GSE17355		GSE162354	
Gene name	logFC	P.Value	logFC	P.Value	logFC	P.Value
Cxcl10	4.420166	1.63E-07	2.396589	0.003769	3.013802	0.000523
Cxcl2	4.107957	1.26E-09	2.530376	0.000555	3.645425	0.016955
Saa3	3.903997	7.83E-08	7.049304	2.26E-11	6.559697	0.000562
Cxcl1	3.468228	2.35E-07	1.607781	0.010081	3.114788	0.006438
Il1b	2.820409	7.66E-08	1.382932	0.046568	3.458001	0.015642
Ifit3	2.615652	2.06E-07	1.650426	2.57E-05	2.01194	0.000238
Ifit2	2.509609	2.13E-06	1.566301	0.000371	1.636927	0.005391
Slfn1	2.479243	3.67E-07	1.362232	0.000357	2.467127	0.044023
Ch25h	2.408337	1.34E-05	1.47822	0.000304	2.605506	0.000638
Serpina3g	2.204735	5.88E-05	2.063319	0.000223	2.397297	0.001629
Casp4	2.124022	3.1E-08	1.00766	6.24E-05	1.25321	0.008079
Mt2	1.884278	2.19E-07	1.306797	0.008776	4.496078	0.005304
Tlr2	1.714867	1.63E-06	2.205383	3.67E-07	2.07476	0.000553
Ctps	1.646085	1.45E-05	1.022879	0.001721	2.119804	1.19E-05
Mt1	1.567044	7.7E-09	1.123028	0.001418	2.446364	0.006295
Ccl2	1.514947	6.74E-06	1.434541	0.006043	3.754432	0.004078
Slfn2	1.502906	5.55E-08	1.351272	0.000618	1.177917	0.005026
Serpina3m	1.489743	1.04E-07	1.60869	0.005604	5.630828	0.000351
Cxcl9	1.488588	0.003916	4.345711	7.06E-07	5.831335	0.000992
Tnfaip2	1.424103	1.09E-07	1.853	4.66E-05	1.652362	0.009195
Lcn2	1.405398	0.000309	3.271	4.3E-06	5.170324	5.03E-05
Timp1	1.392945	1.99E-06	3.338433	5.49E-06	4.401737	0.002089
Sod2	1.330405	4.99E-07	1.383056	3.99E-06	1.196868	0.000694
Snx10	1.31363	1.77E-06	1.356419	2.62E-06	1.493474	0.005628
Tap1	1.274533	0.000156	1.177775	0.001678	1.408763	0.008928
Il1a	1.22931	1.61E-08	1.240222	0.009646	1.099157	0.024313
Pglyrp1	1.2146	0.00073	1.554469	9.9E-05	1.928466	0.003118
Cyp7b1	1.023689	0.000218	1.500844	0.000146	4.58663	0.003869
Serpina3n	1.007102	1.82E-07	1.985278	6.89E-06	2.707062	0.000316